Robustness of interdependent power grid and communication networks to cascading failures

Abdorasoul Ghasemi and Hermann de Meer

Abstract—We consider the cascading failure process in interdependent power-communication networks, where the power grid provides the required energy for the communication nodes, and the communication network facilitates the monitoring and controlling the power networks. The proposed system model considers the flow dynamics in both networks and the failure rollover to study the cascade process in the system and capture the possible beneficial and adverse effects of interdependency between the networks. We suggest weak and strong interdependencies models that determine how and to what extent the loss of controllability after failures impacts the power network and a congestion-aware load balancing scheme that exploits the system state to decrease the density of severe cascades. The results of the cascading failure processes on data from two power networks are provided and discussed in terms of the average unserved load in the power network and the number of failed nodes in the communication layer in different scenarios. We find that increasing the coupling is beneficial in most cases; however, considering the robustness of each network and the nature of the interdependencies between the two networks, over-coupling can decrease the system's robustness against failure cascading in certain scenarios.

Index Terms—Interdependent power-communication network, robustness, cascading failure, coupling coefficient.

1 Introduction

Smart grids emerge to provide the ever-increasing demand for reliable energy using the advances in power systems and communication network technologies. These networks rely on communication networks to monitor, control, and make automatic decision-making in a centralized manner [1] [2]. On the other hand, the elements in a communication network, such as Internet routers and switches, are prone to faults and rely on the energy of the power network and, therefore, depend on the power grid. Accordingly, the modern cyber-physical power grids are considered a kind of interdependent network [3].

Interdependent power-communication networks are expected to generate, transmit, and distribute energy more efficiently, relying on the network's state observability and controllability provided by the communication network [2]. Nevertheless, the fast-growing coupling between two networks is challenging, considering possible adverse effects on interdependent networks' robustness and security. The major blackout of Italy's power grid in 2003 [4] indicates an example of the adverse effects of interdependency on robustness, where the failure rollover between the power and communications layers led to an extensive cascade. The cyberattack on the controlling services of power companies in Ukraine in 2015, which caused a cascading failure, also demonstrates the security risk of interdependencies [5].

The interconnections help improve the system's functioning by optimizing the system's performance using the system's capacity. However, they also open new pathways for failure propagation after unforeseen stresses and make the system more brittle if the network state is lost [6] [7]. This trade-off raises the question of finding the appropriate type and degree of coupling between power and communication networks considering possible failure cascading effects. Since real test on infrastructure networks is not practically possible, and historical data are rare, different modeling is suggested to tackle this question; each captures some peculiarities and details of failure cascading dynamics [8]. Besides, each model provides new insights into designing a robust interdependent power grid network against possible cascading and designing a proper mitigation strategy [9] [10].

Some models focused on structural properties like the connectivity pattern of interdependent networks and exploited the mathematical frameworks like percolation theory [11] or sandpile model [6] to investigate the coupling effects. The authors of [12] have shown that interdependent networks may be more robust to small failures under certain conditions and are more vulnerable to large failures than single-layer networks. Some works conclude that increasing the coupling between two networks decreases the robustness against random failures [13], [14], [15]. Others found non-monotone relationships between the degree of coupling in interdependent networks and their robustness, suggesting that there is an optimal degree for network coupling [16], [17].

Probabilistic models are another class to describe the failure unfolding in interdependent networks. The authors of [18] suggest a generalized probabilistic threshold-based model for failure propagation in intra-and inter-layer. In threshold-based modeling, failure propagates to a node if the number of already affected neighbors exceeds a threshold. Due to the non-local propagation effect of failure

- *A. Ghasemi is with the Department of Computer Engineering, K. N. Toosi University of Technology, Tehran, Iran, E-mail: arghasemi@kntu.ac.ir.*
- *H. de Meer is with the Faculty of Computer Science and Mathematics, Passau University, 94032 Passau, Germany E-mail: Hermann.DeMeer@uni-passau.de.*

Manuscript received January xx, 2021; revised January xx, 2021.

cascading in power grid networks [19], this model could not be applied for the analysis of interdependent power-communication networks.

The structural and probabilistic models explain some aspects of failure cascading in interdependent networks. However, these models overlook the flow of energy and data in the power and communication networks which are crucial factors in failure unfolding [20]. The importance of realistic modeling by considering the nodes' heterogeneity in each layer, the physical constraints in and between layers, and the loading level of the power grid are discussed in [21] [22] [23]. In [24], the authors show that considering the dynamical properties in each power and communication network provides a more accurate cascading failure prediction while incurring the implementation complexities to capture the precise details of the power and communication dynamics.

Taking into account the power grid physical properties [25], [26] as well as the mitigation and controlling role of the communication layer [20], [27], it is found that more coupling between power and communication layers may lead to more robustness against failure events in the corresponding considered power network. These studies, however, do not consider the system constraint due to different possible architectures that define the dynamics of inter-layer cascades between power and communication nodes.

This work studies the robustness of interdependent power-communication networks after an initial random failure imposed on the power layer by removing a random set of links. The failure may cascade in the power layer or roll over to the communication layer degrading the power network's control. We consider a system model that captures the constraints of flow distribution dynamics in the power and communication networks and considers the impact of interdependencies on load balancing decision-making at the control center. The objective is to study how different system constraints induced by considering more realistic dynamics and architecture affect the cascading failure process. Using the developed model, we specifically study how the coupling coefficient and type of inter-dependencies affect the power grids' robustness in terms of the cascading failure size. The main contributions of this study are:

1) The paper introduces and provides the results of two types of weak and strong interdependency models. These models capture to what extent the power network relies on the control center's decisions, affecting the efficiency of decision-making and the system's brittleness in failure cascading. In strong inter-dependency, a power node will disconnect from the network if it loses communication with the control center. In the weak interdependency, however, the control center cannot control this node, i.e., for load shedding of a demand bus or generator tripping of a generator bus, if the communication path between a power node and the control center fails.
2) We suggest a congestion-aware load balancing scheme that considers lines' congestion at the control center for load balancing. Using this scheme, the control center considers the immediate load shedding and the power lines' congestions to select a load balancing strategy according to the current controllability state. We show that by considering the power lines' boundaries, one can decrease the average unserved load ratio in both strong and weak models while the density of small and medium cascades increases and the density of severe ones decreases.
3) We show that depending on the interdependency model and the robustness of each network, there are scenarios in which the adverse effects of interdependency may be dominant, making the interdependent system less robust to random failure.

In the following, Section 2 presents the system model of the interdependent power-communication network. Section 3 describes how failures cascade within each layer. In Section 4, we first explain the inter-layer failure cascading and introduce strong and weak interdependency models. Here, we also present the congestion-aware load balancing scheme at the control center. Section 5 defines the metrics used for evaluating the performance of the interdependent system after initial random failures. In Section 6, we simulate the cascading failure process on the interdependent power network based on the introduced system model and load balancing strategy for diverse cascading scenarios and discuss the results for robustness evaluation. Finally, the paper is concluded in Section 7.

2 System model

We consider a two-layer interdependent power-communication network that uses a control center to monitor and control the power buses via receiving and sending control signals for proper load balancing after possible failures. See Fig. 1.

Let $G_P = (\mathcal{V}_P, \mathcal{E}_P)$ describe the power network, where $\mathcal{V}_P$ is the set of power nodes or buses, and $\mathcal{E}_P$ is the set of power edges or lines. We use the terms buses and lines to refer to the power graph in the rest. We denote the total number of buses and lines of G_P by n_P and m_P, respectively. The power demand and generation vectors are denoted by $\mathbf{p}_D$ and $\mathbf{p}_G$. We use the DC power flow distribution model described in section 3.2 to calculate the flow, f_{ij} on line $e = (i, j)$.

The control center monitors and controls the power grid's nodes via the communication network in a centralized manner. The communication layer C consists of several routing nodes, where we assume that the routing node with the highest betweenness centrality is directly connected to the control center [28]. We describe the communication network by graph $G_C = (\mathcal{V}_C, \mathcal{E}_C)$, where $\mathcal{V}_C$ is the set of communication nodes and $\mathcal{E}_C$ is the set of communication links between the communication nodes. We use the terms nodes and links to refer to the communication graph in the rest. We use the Motter-Lai model for the data flow distribution in the communication network, as we explain in Section 3.1. The communication network has the same number of nodes as the power network, and its topology is synthesized based on the corresponding power network's topology as explained in section 6.

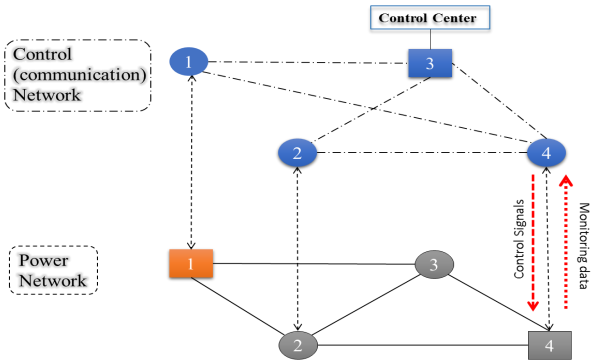

Fig. 1: The structure of the interdependent power-communications network is shown. The power grid consists of power-generating buses (square) and power-consuming buses (circle). A cyber bus connects to the control center via a communication node, and a coupled communication node gets electrical energy from the corresponding bus.

A subset of buses is selected randomly and uniformly according to the coupling coefficient, q, and couples the power network to the communication network. We considered a one-to-one interdependency model, in which each bus is only connected to a single corresponding node in the communication layer and vice versa. We refer to coupled buses as cyber buses. The rationale for using this interdependency model is that the power networks and the corresponding communication layer are typically co-evolved over time, i.e., when a should-be observable or controllable bus is added to the power network, the corresponding communication node is also created.

Let i be a cyber bus. The Control center can monitor and send actuating signals to i if there is a route from the control center to the corresponding communication node of i. Also, the coupled node j in the communication layer relies on the energy and functions if the corresponding bus remains connected to the power network. Therefore, the number of codependent performance buses or nodes in each layer is $q \times n_P$.

The control center in this interdependent system attempts to rebalance the network's power supply and demand after a failure. The failure is imposed in the transmission lines and may cascade through the power network, disconnect the network's topology, and propagate to the communication layer. The failure propagation models within the power and communications networks are discussed in detail in Section 3, and the interlayer cascading model is presented in 4.1. To ensure the load balancing and mitigate the cascade, the control center may shut down some power nodes relying on the communication network to send appropriate control signals, as discussed in subsection 4.2.

3 CASCADING FAILURE PROCESS

The cascading failure process in an interdependent power network consists of three sub-processes: (i) cascading within the Power grid, (ii) cascading within the communication layer, and (iii) inter-layer cascading. The process starts with a random initial line failure in the power network. According to the flow redistribution model, the initial failure leads to flow changes on other lines. The failure may propagate to the communication layer if a coupled node loses its connection to the power network, i.e., the corresponding coupled bus in the power network is isolated. The flow redistribution at the communication layer may lead to consecutive failures if a node's load exceeds its capacity. Hence, a coupled communication node may fail either by losing its connection to the power network or possible overloading after a rerouting.

We use flow redistribution models to study how cascades unfold in the power and communication networks. The flow-redistribution models capture the cascading process's main features and are proper models for describing the cascading failure process in flow networks such as power grids and communication networks [8]. In flow-redistribution models, the failure of a fraction of lines (in the power network) or nodes (in the communication network) redistributes the flow of energy or data to other lines or nodes, which puts the system in a new state. If the load on a line or a node exceeds its capacity, it will fail, causing another redistribution of loads in the corresponding network. The process will continue until the system reaches a steady state and no more failure happens. In the following, we provide the details of the adopted model for each subprocess.

3.1 communication layer

The data flow between the coupled nodes and the control center may change after a node failure in the communication layer. This initial failure may occur accidentally, due to a lack of power source, or even due to cyber attacks [9], [29]. We use the Motter-Lai flow redistribution to model node failure cascading in the communication layer [30]. Here, the initial node failure event is imposed on the communication network after a coupled bus failure in the power network. The initial failure changes the shortest paths between coupled nodes and the control center, altering the data flow distribution and may cause subsequent secondary node failures. Secondary node failures are because of possible congestion after flow redistribution. When the offered load exceeds the node's capacity, the traversing packets incur excessive delay, making communications nonfunctional. Therefore, the routing strategy does not consider the congested nodes in pathfinding. The failure cascading unfolds until no more nodes is failed.

The node's capacity depends on each node's normal operation initial load. To estimate the working load of each node, we assume that in the normal operation of the communication network, a unit of information communicates between node pairs at each time step through the shortest path. Therefore, the load on node j is the total number of shortest paths that pass through it given by its betweenness centrality and denoted by L_j. The capacity of node j, L_j^{max}, is proportional to its initial load, L_j^0 and is given by

$$L_j^{max} = (1+\beta)L_j^0, \quad \forall j \in \mathcal{V}_C, \tag{1}$$

where $0 \leq \beta \leq 1$ is the tolerance coefficient, which determines the tolerance of nodes against overload. The ratio-

nale behind this model lies in the non-linear relationship between the average incurred delay and the load on the node's output link, in which if the offered load exceeds a saturation point, the incurred delay increases abruptly. See supplementary material for more details about this model.

3.2 power layer

We use the DC model for flow distribution and redistribution after failure in power grids, which is widely used for cascading failure analysis in transmission power networks [25], [31], [32]. This simple model has good stability in describing overload-based failures and provides a good estimate of the power flow distribution process, close to reality [33], [34]. In this model, the voltage phases of the buses are given by [4], [35]:

$$\mathbf{L}\boldsymbol{\theta} = \mathbf{p}_G - \mathbf{p}_D, \tag{2}$$

where $\boldsymbol{\theta} = (\theta_1, \ldots, \theta_{n_p})$ is the vector of buses' phases. Matrix $\mathbf{L}$ is the Laplacian matrix of the $\mathcal{G}_p$, i.e., $L_{ij} = -b_{ij}$ if there is a link between i and j, and $L_{ii} = -\sum_j b_{ij}$ where b_{ij} is the susceptance of link (i, j). Having the voltage phases, the flow of link (i, j) is then given by

$$f_{ij} = b_{ij}(\theta_i - \theta_j). \tag{3}$$

Since the total power generation and demand must be equal, $\mathbf{1}^T(\mathbf{p}_G - \mathbf{p}_D) = 0$, there are $n_p - 1$ unknown voltage phases in the linear set of equations (2) and (3). Practically, the voltage angle of a specific generator bus called the slack generator is considered zero, and its power generation adjusts to meet the supply-demand balance in the network. We select the generator bus with the maximum unused generating power as the slack bus and index this node by s. Generators' maximum possible power generation is also denoted by $\mathbf{p}_{G-max}$.

For each transmission line $e = (i, j) \in \mathcal{E}_\mathcal{P}$, we define $f_e = |f_{ij}| = |f_{ji}|$ and f_e^{max} as the power flow and maximum flow capacity of the line e respectively. If the power flow on the line e exceeds its maximum flow capacity, i.e., $|f_e| > f_e^{max}$, the line fails and will be removed from the network. This failure changes matrix $\mathbf{L}$; consequently, the voltage phases and lines' flows change. This alternation of flows on the transmission lines may cause new overloads, triggering cascading failures within the power network [36].

See Algorithm 1 for the details of the iterative cascading failure process. Let $S_t \subseteq \mathcal{E}_P$ denote the set of failed edges in the t_{th} iteration of the cascading process. Also, for $t \geq 1$, $S_t^* = S_{t-1}^* \cup S_t$ is the set of failed edges at the end of iteration t. We assume that before the initial failure events $S_0 \in \mathcal{E}_P$, the links are not overloaded, $|f_e| \leq f_e^{max}, \forall e \in \mathcal{E}_P$. The isolated nodes and those whose demanding power shut down during the cascading process are considered failed nodes. At the end of t_{th} iteration of the cascading process, the set of failed nodes is denoted by $U_t \subseteq \mathcal{V}_P$. Due to the possible link failure, the network may decompose into several connected components at iteration t. Let k be the number of connected components after removing the failed edges S_t^*. Also, assume $G_P^t = \{\mathcal{G}_0^t, \mathcal{G}_1^t, ..., \mathcal{G}_k^t\}, k \leq n_P$, is the set of the corresponding components. For connected component $\mathcal{G}_k^t = (\mathcal{V}_k^t, \mathcal{E}_k^t)$, we have $\mathcal{V}_k^t \subseteq \mathcal{V}_P$ and $\mathcal{E}_k^t \subseteq \mathcal{E}_P \setminus S_t^*$.

The process starts with checking the possible power imbalance in each connected component. If $\mathcal{G}_k^t$ contains a single node or does not include a generator node, all of the component's nodes are assumed to be failed and added to U_t. Next, the load balancing mechanism is called. Here, the control center helps decide which loads should be shut down and which generators tripped, relying on the state information provided by the communication layer. We will discuss the congestion-based load balancing scheme and the power-communication interactions shortly.

We add the power nodes that are shut down during the load balancing process to the failed nodes set U_t. Next, for a balanced power component, we consider one of its generators as the slack bus, solve the DC equations (2) and (3), and compute the power flow on the component edges. Let $f_e(S_t^*), e \in \mathcal{E}_P \setminus S_t^*$ denote the new computed flow of edges in G_P^t after edge failures $S_t^* \subseteq \mathcal{E}_P$. We check the possible transmission link overloads in G_P^t, and if there is an overload on edge e, this edge is added to the failed edges list S_t. The cascading process steps run iteratively until the list of failed edges S_t is empty, and the power network reaches a state with no overloaded link in $G_P^{t_\infty}$.

Algorithm 1 Cascading failure process in power network

Input:
$G_P(\mathcal{V}_P, \mathcal{E}_P)$: connected power network
$S_0 \subseteq \mathcal{E}_P$: initial edge failure events
$\mathbf{p}_G$: list of generator nodes
$\mathbf{p}_D$: list of consumer nodes
$\mathbf{p}_{G-max}$: list of maximum generations of all power nodes
Output:
$G_P^{t_\infty}(\mathcal{V}_P^{t_\infty}, \mathcal{E}_P^{t_\infty})$: power network after cascading
$U_t \subseteq \mathcal{V}_P$: set of failed nodes
$S_{t_\infty}^* = (S_0, S_1, ..., S_{t_\infty})$: sequence of failed edges after the initial event S_0

$t \leftarrow 0$ ▷ initial state
$S_0^* \leftarrow S_0$ ▷ initial edge failure events
while $S_t \neq 0$ **do**
  $G_P^t = (\mathcal{V}_P, \mathcal{E}_P \setminus S_t^*)$ ▷ Apply edge events in S_t
  Compute $\mathcal{G}_P^t = \{G_0^t, G_1^t, ..., G_k^t\}$ ▷ find connected components
  $r \leftarrow 0$
  for $G_r^t, \forall r \leq k$ **do**
    if $|\mathcal{V}_r^t| = 1$ **or** no generator in G_r^t **then** ▷ the component contains no generator or is a single node
      $U_t \leftarrow U_{t-1} \cup \mathcal{V}_r^t$ ▷ component's nodes are failed
    else
      Call load balancing mechanism ▷ interaction with communication layer
      $U_t \leftarrow U_{t-1} \cup \{u | p_D^{(u)} = 0, \forall u \in \mathcal{V}_r^t\}$ ▷ add new shedded nodes to U_t
      Compute new flows $f_e(S_t^*), \forall e \in \mathcal{E}_r^t \setminus S_t^*$ using DC power flow equations and update (2) and (3)
    $r \leftarrow r + 1$
  $S_{t+1} = \{e | f_e(S_t^*) > f_e^{max}, e \in \mathcal{E}_P \setminus S_t^*\}$ ▷ find the set of new edge failure events
  $S_{t+1}^* \leftarrow S_t^* \cup S_{t+1}$
  $t \leftarrow t + 1$

The load balancing decisions impact the cascade process and may prevent or mitigate its effects [37], [38], [39]. The load balancing mechanism uses load shedding and generator tripping to manage significant power imbalance in each component [40]. Nevertheless, there might be different solutions, pushing the system into a new state that might be less brittle to possible consecutive stresses. Also, the decision could be made in a decentralized or centralized

manner [41]. The decentralized schemes operate based on local information, such as measured DC voltages, and do not rely on a central control decision.

Under-frequency load shedding (UFLS) and under-voltage load shedding (UVLS) are two techniques for decentralized load balancing [38]. UFLS scheme detects generation deficiencies within each component and sheds the minimum load until nominal frequency recovery. The UFLS scheme is inefficient if voltage collapse occurs within the island. Voltage instability stems from reasons such as the overloading of transmission lines and generator failures. The UVLS scheme restores voltage to its nominal value by sequentially shedding the low-priority loads whose observed voltage drops below a predefined threshold when higher thresholds are assigned to high-priority loads [41]. A common practice in decentralized load balancing schemes is removing the least significant loads from the network, based on previously recorded data and preset defaults, to the extent that the balance between generation and demand is established [40]. Therefore, the low-priority loads, the voltage thresholds, and the amount of load shedding are determined based on previous experience or simulated data. These strategies best suit single-layer power grids with geographically scattered loads across the network. Furthermore, these strategies do not consider the possible consequences of their responses on the whole system and its robustness to possible future stresses. The centralized schemes, on the other hand, use the communication layer to monitor and send appropriate control signals and, looking ahead, mitigate the possible cascade, as we shall discuss in Section 4.

4 INTERDEPENDENT POWER-COMMUNICATION NETWORKS

The communication network facilitates power network management by observing the network state, finding optimal strategies, and sending control signals online [42], [43]. For example, a centralized load balancing scheme uses the communicated network's state in its decision to compute and send appropriate actuating load shedding or generator tripping in case of significant disturbances after a random line failure. The centralized strategy advantages are high controllability, shedding the optimal loads, and considering possible secondary failures during the cascading process [44]. However, the underlying interdependency to the communication network imposes further constraints on the system and may adversely affect the whole system's robustness. For example, there might be possible failure propagation between the networks, which leads to inter-layer failure rollover. Furthermore, it is crucial to determine to what extent the operation of each layer depends on the other. That is, how failure propagates from one layer to the other and how the control center and cyber buses should respond in the case of partial observability. This section presents a system model that captures interdependency's beneficial and potential adverse effects to draw new insights for future energy networks.

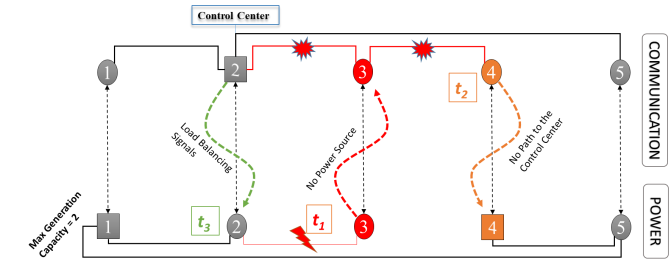

t_0	2	-1	-1	2	-2
t_1	1	-1	0	2	-2
t_2	3	-1	0	0	-2
t_3	2	0	0	0	-2

Fig. 2: The figure shows a cascading failure process in a strong interdependent power-communication network. The power nodes' loads at each time step are listed in the table below. The cascading process begins with the failure of the edge between nodes 2 and 3 at t_0. Next, node 3 disconnects from the power grid and shuts down. In t_1, node 3 of the communication layer fails, and its connected edges are removed due to a lack of power source. In t_2, due to the communication node 4 failure and isolation, the corresponding generator node 4 in the Power layer shuts down. In t_3, the power network load is imbalanced. The control center could not increase the generation power of node 1 as it goes beyond its capacity. Consequently, the control center shuts down the load on node 2 to mitigate the cascading failure process.

4.1 inter-layer cascading

We start with the dependency model of the communication network to the power network. Recall that a certain fraction of communication nodes are coupled in a 1-to-1 manner to the corresponding cyber buses in the power network. We assume that a coupled communication node, e.g., a router, functions appropriately if the corresponding dependent cyber bus in the power layer functions appropriately. If the corresponding power node fails, the communication node and the inter-layer edge also fail. We select the node with the greatest betweenness centrality as the control center in the communication network and assume that the control center node is not affected by failures in the power system. The control center can observe and control a cyber bus if the corresponding communication node is working and there is at least one communication path between this node and the control center.

We consider two models for power-communications interdependency; each imposes different pros and cons. The first one is called weak dependency, in which the lack of a communication path between the cyber bus and the control center makes this bus unobservable. Therefore, the imperfect operation of the communication layer leads to partial observability and controllability of the power network; hence, the solution space is limited in finding a load balancing strategy. Here, the uncontrollable cyber bus functions as a fixed load or generator. Therefore, the decoupled cyber buses are weakly dependent on the communication layer but impose more constraints on finding an optimal strategy in the control center if there are any irregularities.

The second dependency model is called strong dependency. In a strong dependency type, however, the cyber bus function relies entirely on the existence of a communication path to the control center. The cyber bus is disconnected from the power network if it does not receive the control signal from the control center, increasing the immediate load shedding after failures. On the other hand, the control center may make a better decision in future steps because it does not constrain by fixed loads or generations.

The cascading failure process in the interdependent power network is simulated in consecutive steps. The initial disturbance is applied by removing a fraction of the power network edges. In the next step, this failure may cascade within the power network according to Algorithm 1. Also, the failure may roll over to the communication network through dependency edges. Note that in Algorithm 1, we use the congestion-based load balancing strategy in which the control center can control the supply/demand of the connected nodes through the communication network. In the case of strong interdependency, the communication node failure may roll over to the power network and lead to new failures within the power network, and the process runs iteratively until no new failure happens in the power and communication network. If the control center fails to balance the network using the observable cyber buses, all buses in the unbalanced component will fail. In figure 2, we provide an illustrative example of this inter-layer failure cascading, where a failure in the power network leads to consecutive failures in the power and communication networks.

4.2 centralized congestion-aware load balancing

In an interdependent power-communication network, the control center is in charge of automatically computing and making optimal decisions to maintain the network performance after disturbances. The most crucial decision is load balancing, in which the control center decides load shedding and/or generator tripping in each component if necessary.

The straightforward solution is minimizing the immediate amount of unserved load after the initial failure, considering the physical constraints, particularly the capacity limit of lines. Increasing the coupling coefficient, q, improves the power network controllability as it provides more degrees of freedom in the control center to balance the power network. However, it also provides new pathways for failure propagation between layers that make the system brittle after random failures affecting the control pathways. Aiming to minimize the unserved load and meet all constraints, the control center can not find a feasible solution in some scenarios, or it may find solutions that utilize the power lines near their capacities, making them more brittle in the subsequent flow redistribution.

This section discusses that after an initial failure in the power layer and its impact on the communication layer, the control center may have limited degrees of freedom to find a feasible solution as it may lose access to cyber buses. In the proposed congestion-aware load balancing, the control center considers both the immediate shedding load and congested power lines in load balancing. That is, instead of considering a hard limit for lines' capacities that divides all possible load balancing solutions into feasible or non-feasible solutions to the optimization problem, we can distinguish between balancing strategies according to how they challenge the system boundaries. We show by extensive simulation that by selecting a strategy that considers slack capacity over lines or extending the solution space to violate the capacity limits of some lines with proper costs in the optimization process, we can find balancing strategies that decrease the frequency of severe cascades and even improve the average unserved load ratio.

Let $\mathcal{V}_P^t \subseteq \mathcal{V}_P$ denote the set of power nodes with at least one path to the control center at time step t of the cascading process. We assume that the control center has the necessary information about the power nodes and edges to which it has at least a path through the communication layer. Define two binary variables X_i and Y_j. $X_i = 1$ indicates tripping the power generation at node i for $i \in g - \{s\}$ where $g \subset \mathcal{V}_P^t$ is the set of observable generators which are connected to the control center through communication layer, and s is the index of the slack generator. $\mathbf{X}$ is the vector of corresponding decision variables. Recall that the power generation at s, $p_G^{(s)}$, is a variable used to meet the constraints of DC power flow equations (2) and (3). Accordingly, $Y_j = 1$ indicates shedding the load at node j for $j \in \mathcal{V}_P^t$ and $\mathbf{Y}$ is the corresponding decision vector.

Also, let continuous variable Z_e denote the amount of overload on line $e, e \in \mathcal{E}_P^t \subseteq \mathcal{E}_P$, i.e., if the absolute value of the power flow on the transmission line e, $|f_e|$ is greater than a fraction of its capacity, $\mu_1 f_e^{max}$ and $0 \leq Z_e \leq (1 - \mu_1 + \mu_2) f_e^{max}$ where $0 < \mu_1, \mu_2 < 1$ are selected constants. The overload cost of line e, C_e, is given by:

$$C_e = \begin{cases} P_1 Z_e & if\ 0 < Z_e \leq (1-\mu_1)\, f_e^{max} \\ P_2 Z_e & if\ \ (1-\mu_1)\, f_e^{max} < Z_e \end{cases} \tag{4}$$

where $P1, P2$ are the costs of approaching the capacities of the lines beyond the specified threshold $\mu_1 f_e^{max}$ and violating the capacity constraint. The control center balances the power network by control signals $\mathbf{X}$, $\mathbf{Y}$, and tuning the power generation of the slack bus $p_G^{(s)}$ considering both the current demand shedding and the cost of overloaded lines.

The formal optimization problem for load balancing in the two-layer power-communication network is given in (5a)-(5o).

$$\min_{\mathbf{X},\mathbf{Y},\mathbf{Z},\boldsymbol{\delta^1},\boldsymbol{\delta^2},p_G^{(s)}} \sum_j p_D^{(j)} Y_j + \sum_e C_e \tag{5a}$$

subject to

$$|p_G^{(s)} + \sum_i (1 - X_i) p_G^{(i)} - \sum_j (1 - Y_j) p_D^{(j)}| = 0, \tag{5b}$$

$$p_G^{(s)} \leq p_{G-max}^{(s)} \quad s \in g, \tag{5c}$$

$$|f_e| - \mu_1 f_e^{max} \leq Z_e, \quad \forall e \in \mathcal{E}_P^t, \tag{5d}$$

$$Z_e \in \big[0, (1 - \mu_1 + \mu_2) f_e^{max}\big], \quad \forall e \in \mathcal{E}_P^t, \tag{5e}$$

$$Z_e - (1 - \mu_1) f_e^{max} \leq M(1 - \delta_e^1), \forall e \in \mathcal{E}_P^t \tag{5f}$$

$$C_e - P_1 Z_e \geq -M(1 - \delta_e^1), \forall e \in \mathcal{E}_P^t, \tag{5g}$$

$$C_e - P_1 Z_e \leq M(1 - \delta_e^1), \forall e \in \mathcal{E}_P^t, \tag{5h}$$

$$Z_e - (1 - \mu_1) f_e^{max} \geq -M(1 - \delta_e^2), \forall e \in \mathcal{E}_P^t, \tag{5i}$$

$$C_e - P_2 Z_e \geq -M(1 - \delta_e^2), \forall e \in \mathcal{E}_P^t, \tag{5j}$$

$$C_e - P_2 Z_e \leq M(1 - \delta_e^2), \forall e \in \mathcal{E}_P^t, \tag{5k}$$

$$\delta_e^1 + \delta_e^2 = 1, \quad \forall e \in \mathcal{E}_P^t, \tag{5l}$$

$$X_i \in \{0, 1\}, \quad \forall i \in g - \{s\}, \tag{5m}$$

$$Y_j \in \{0, 1\}, \quad \forall j \in \mathcal{V}_P^t \tag{5n}$$

$$\delta_e^1, \delta_e^2 \in \{0, 1\}, \forall e \in \mathcal{E}_P^t, \tag{5o}$$

where M is a large constant.

The objective function in (5a) minimizes a weighted cost of the immediate load shedding and the amount of overload on lines. Constraint (5b) ensures rebalancing and the conservation condition. The maximum power generation of the slack bus generator, $p_G^{(s)}$, is constrained by (5c).

Constraint (5d) is a soft limit for each line capacity, and Constraint (5e) limits the amount of overload on each line. (5d) and (5e) ensure that $Z_e > 0$ if and only if $|f_e| > \mu_1 f_e^{max}$. δ_e^1 and δ_e^2 are binary auxiliary variables for each line that show the overload amount. If $\delta_e^1 = 1$ and $\delta_e^2 = 0$, (5f) ensures that $Z_e \leq (1 - \mu_1) f_e^{max}$ and (5g)-(5h) sets $C_e = P_1 Z_e$. In this case constraints (5i)-(5k) are inactive. If $\delta_e^1 = 0$ and $\delta_e^2 = 1$, (5i) ensures that $Z_e > (1 - \mu_1) f_e^{max}$ and (5j)-(5k) sets $C_e = P_2 Z_e$. In this case constraints (5f)-(5h) are inactive. Finally, (5l)-(5o) show the range of optimization binary variables.

Applying the load balancing based on solving optimization (5a)-(5k), the control center favors solutions that retain enough slack capacity on lines for possible future stresses. Also, by allowing us to go beyond the line capacity, it tries to decrease the infeasible scenarios as we have to shed all loads and trip all generators in the corresponding component in infeasible scenarios.

Note that as a special case, if we set $\mu_1 = 1, \mu_2 = 0$ we have $Z_e = 0$ and hence $C_e = 0$, reducing the problem to the classic optimization of minimizing the immediate load shedding. Also, the auxiliary variables δ_e^1, δ_e^2 for line e allow having different penalties for overloads that are still below the line capacities and the cost of violating the line e capacities and accepting its failure. However, it also increases the number of decision variables in the optimization problem, which makes it more time-consuming.

5 PERFORMANCE METRICS

There are different metrics to measure the interdependent power network robustness in the cascading failure processes. The most important metric for evaluating the cascade effect on the power network is the ratio of unserved load to the network's total load in regular operation as [45]:

$$ULR_f = 1 - \frac{\sum_i p_{D-end}^{(i)}}{\sum_{i \in \mathcal{V}_P} p_{D-0}^{(i)}}, \tag{6}$$

where $\sum_i p_{D-0}^{(i)}$ is the total demanding power of all consumers before the initial failure and $\sum_i p_{D-end}^{(i)}$ is the total demanding power load, served at the end of the cascading failure process. ULR_f determines the relative size of the power lost due to the initial failure of a fraction $f \in [0, 1]$ of power grid edges.

Giant component size is the ratio of the number of nodes in the final remaining connected giant component, n^{GC}, to the total number of nodes, $P_\infty = n^{GC}/n_P$ [3]. This metric reflects the cascade effects on the connectivity of the network. The size of the giant component is the main objective in structural cascading failure analysis.

We measure the cascade effect on the communication layer by the ratio of failed communication nodes $C_\infty^f = n_C^{failed}/n_C$, where n_C^{failed} is the total number of failed nodes within the communication layer at the end of the cascading failure process.

We measure the power to communication failure rollover ratio PCR by finding the ratio of the number of failed communication nodes due to the failure of the corresponding node in the power layer during the interdependent cascading process, n_C^{df}, by

$$PCR = n_C^{df}/n_C, \tag{7}$$

In the case of strong interdependency, we also find the communication to power failure rollover ratio CPR, which determines the ratio of the number of shutting down buses, n_P^{df}, due to the loss of communication with the control center during cascading failures by

$$CPR = n_P^{df}/n_P, \tag{8}$$

PCR and CPR metrics depend highly on the q because they only measure the dependent failed nodes' ratio.

6 SIMULATION RESULTS AND DISCUSSIONS

We first study how considering the lines' congestion in load balancing can help find better solutions and decrease the unserved load ratio in the interdependent system model. Next, we discuss the impact of power network observability on the robustness of the interdependent power network in strong and weak models for different fractions of random line failures and compare it to the full observable scenario. Finally, considering different interdependency types, we investigate the coupling effect on the final cascade size.

We simulate and present the results on IEEE-118-Bus and IEEE-300-Bus transmission networks. The required data, including the network connectivity, the lines' capacities, and the maximum generators' powers, are available in [46]. Due to the high lines' reactance to resistance ratio values, we can use DC power flow to compute the lines' flows. The basic statistics of these networks are summarized in table 1. These data sets also provide the admittance values and the maximum transmitting power of the transmission lines. We have generated different instances of the original power network for simulation purposes by modifying the original power generation and demand values to consider the demand variations over time.

TABLE 1: Basic statistics of the studied power networks: total number of nodes n_P; the total number of edges m_P; mean degree $\langle k \rangle$; mean distance between connected node pairs $\langle l \rangle$; clustering coefficient C and network's diameter d.

Networks	n_P	m_P	$\langle k \rangle$	$\langle l \rangle$	C	d
118-Bus	118	179	3.034	6.26	0.136	14
300-Bus	300	409	2.72	9.90	0.096	24

In each simulation setup and to consider load variations, we generate new instances of the corresponding power network from the reference data. For this purpose, we calculate the demanding load ratio to the maximum possible generating load in the reference sample of each network. We generate a new instance by randomly increasing the generation and demanding loads in different nodes so that the resulting scenario is balanced and no transmission line is overloaded.

The corresponding communication network for each power network instance has the same number of nodes, and its topology is generated by randomly rewiring 10% of the power network and randomly adding 10% more edges to this graph. The capacity of each node in communication networks is determined using the Motter-Lai equation (1), according to the initial load on it and the tolerance parameter β of the network. Other details of each simulation setup are given in the corresponding subsection.

6.1 Congestion aware load balancing

We first discuss the importance of considering line congestion in the centralized load balancing scheme using penalties $P_1 = 1$ and $P_2 = 10$ in optimization problem (5a)-(5o). We generate 5 instances of the IEEE-118 power network, consider 5 random rewiring between the layers, and measure the unserved load ratio for a pre-determined 100 random line failure scenarios with $q = 0.5$, $\beta = 0.3$, and $f = 0.05$.

We perform extensive simulations and study the behavior of the cascading process on the interdependent power-communication network for different values of μ_1 and μ_2. Fig. 3 shows the density function of the corresponding ULR for congestion aware load balancing ($\mu_1 = 0.8, \mu_2 = 0.4$) against the scenario which does not consider lines' congestions ($\mu_1 = 1.0, \mu_2 = 0$) for strong and weak interdependent models. In both models considering the lines' congestions in the load balancing decreases the average unserved load by decreasing the density of severe cascades. Here for the strong model, the ULR is decreased from 0.35 to 0.31, and for the weak interdependency model, from 0.30 to 0.25.

We perform this simulation over different random initial failure sets, inter-layer rewiring, different values of β and q, and observe the same behavior for both weak and strong interdependency models. The average unserved load ratio decreases while the density of low to medium cascades increases, and the density of severe cascades decreases. We also observe the same trend for the IEEE-300-Bus network. See Fig. S1 in the supplementary material file.

We also perform this simulation when we set $P_1 = P_2$ and observe the same behavior while the improvement in the average unserved load ratio is decreased. That is, by removing the $\boldsymbol{\delta^1}, \boldsymbol{\delta^2}$ vector variables from the optimization, we can still find a better solution compared to the case that we do not consider lines' congestions.

These results suggest that interdependent power-communication networks can take advantage of network observability and controllability for automatic decision-making of load balancing at the control center. Also, by considering the lines' congestions, decisions can be made such that we can avoid the possible brittleness due to underlying interdependency consequences in random failures.

6.2 Robustness against random failures

This section evaluates the robustness of interdependent power-communication networks against random failure cascading. Here, to run the simulations over enough samples timely, we set $P_1 = P_2$. We simulate the cascading failure process by randomly removing a fraction f of lines in the power network and measuring the ULR. We also report the size of the giant component P_∞.

The result for each f is the average of running the process for 5 instances of power network at different loads and 5 instances for the corresponding communication network. We randomly chose 5 distinctive sets of couplings between the nodes of two layers for each pair of these power and communication networks according to the coupling coefficient q to construct the interdependent network. Finally, we simulate the process 10 times by randomly removing a fraction f of lines. Accordingly, the results are the average of 1250 distinct scenarios with different loads, communication network topologies, coupling patterns, and failure scenarios for each point. We find that this sample size provided a reasonable tradeoff between the confidence interval and required computational time, which is significant given the details of our model.

We provide the corresponding results of a fully observable network in which all buses are considered cyber buses and observable by the control center. The gap between an interdependent and the full observable scenario shows the adverse effect of interdependency and controllability loss in the strong model and controllability loss impact in the weak model.

Fig. 4 show the unserved load ratio and giant component size for the strong and weak models for $\beta = 0.3$ and different values of coupling coefficients. We first note that the full controllability of the power network, as expected, helps in optimal decision-making, and losing that degrades

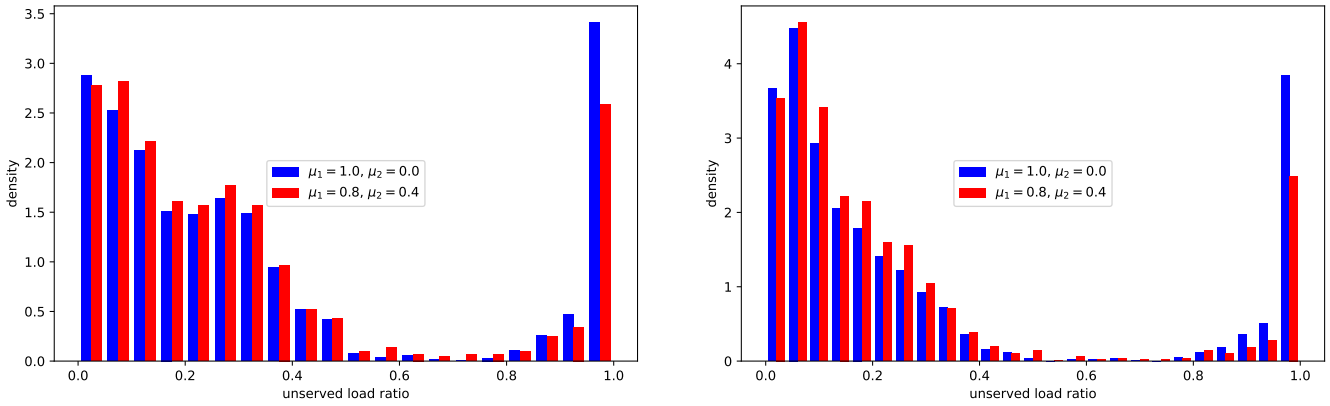

(a) (b)

Fig. 3: The density function of the unserved load ratio without ($\mu_1 = 1.0, \mu_2 = 0$) and with ($\mu_1 = 0.8, \mu_2 = 0.4$) consideration of lines congestions for (a) strong interdependency and (b) weak interdependency models.

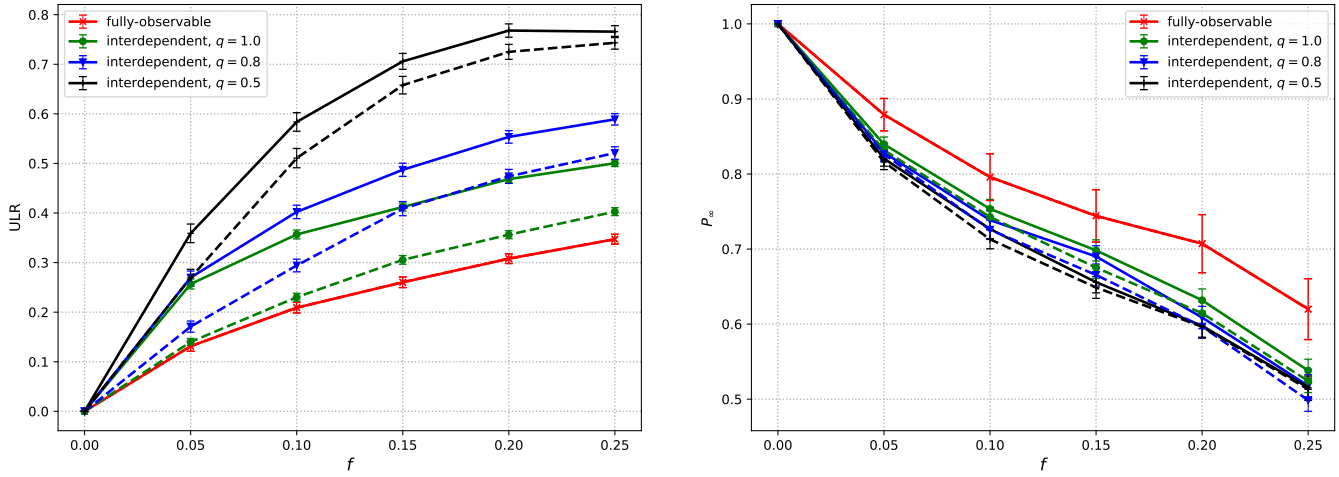

(a) (b)

Fig. 4: The average and the corresponding 95% confidence interval of (a) ULR and (b) giant component size P_∞, against the fraction of randomly failed edges for the IEEE-118-Bus for $\beta = 0.3$. The dashed lines are for the weak model, and the solid lines are for the strong model.

the desired performance metrics, especially in the strong dependency model. Also, Fig. 4a shows that the ULR increases rapidly if the coupling coefficient decreases, especially in the strong interdependency model. Furthermore, Fig. 4b shows that the size of the giant component does not change in different scenarios. We observe the same trend for the IEEE-300-Bus network. See Fig. S2 in the supplementary material file. This result suggests that strong and weak dependency may degrade the robustness by more interlayer failure propagation and decrease the control center's ability to mitigate cascade effects.

We also note that increasing the coupling coefficient is beneficial when the fraction of lost lines f is large enough, $f > 0.05$. We investigate the impact of the coupling coefficient for small values of f in the following subsection.

6.3 The effect of coupling coefficient

We simulate and measure the ULR for the IEEE-118-Bus network to investigate the impact of the coupling coefficient on the interdependent power for small values of f.

Fig. 5a shows the ULR metric after removing a fraction $f = 0.05$ of edges in the IEEE-118-Bus grid for different values of q and $\beta = 0.1, 0.3$. In the weak model, depicted by dash lines, we see a monotonic decrease in the ULR as the coupling between the two networks increases suggesting that the power network's robustness increases. The reason is that with the increase in the number of edges between the two networks, the power network controllability through the communication network is increased; therefore, the control center better mitigates the effects of the cascade. In contrast, in the strong interdependency model depicted by solid lines, we observe that increasing the coupling beyond a

threshold is not beneficial or increases the ULR. This feature is highlighted more for smaller values of β, i.e., when the communication layer is not robust enough. The reason roots in the adverse effect of communication on power failure rollovers. See Fig. 5b. We observe the same pattern for the IEEE-300-bus network. See Fig. S3 in the supplementary material file.

In the strong interdependency model, by increasing q, the CPR may increase rapidly, canceling the gain of increasing controllability, especially for low values of β. This result is consistent with previous results for pure structural models, which suggested that increasing the coupling coefficient beyond a threshold has an adverse effect and decreases the system's robustness.

This result suggests that the interdependent power network's robustness may decrease beyond a coupling coefficient threshold consistent with the pure topological models. This threshold depends on the β, as for large values of β, the number of communication to power rollovers decreases significantly.

Finally, Fig. 6 shows the effect of the coupling coefficient on the robustness of the communication layer against failure cascading in the interdependent power grid. Fig. 6a and Fig. 6b show, respectively, the total fraction of failed communication nodes and the fraction of failed nodes due to the failure rollover from the power network.

We note that by increasing q, more communication nodes are susceptible to failure as their corresponding cyber bus may fail. On the other hand, by increasing q, we expect an increase in the power network controllability that better mitigates the initial failure effects by the control center.

Fig. 6a and Fig. 6b show that for $\beta = 0.1$, the total fraction of failed communication nodes and the fraction of power to communication failure rollovers increases in both weak and strong interdependency models. However, for $\beta = 0.3$, increasing the coupling coefficient beyond a threshold, i.e., $q > 0.4$, is beneficial as the total number and the fraction of power to communication failure rollovers decrease. From the communication layer perspective, increasing the coupling is beneficial when this network robustness is sufficiently large. See Fig. S4 for the results of the IEEE-300-bus network.

These results suggest that interdependency could benefit interdependent power-communication networks under certain conditions. The main factors that impact different system performance metrics are the interdependency model, the interdependent decision-making load balancing, the robustness of each layer, and the coupling coefficient.

7 Conclusion

We proposed a system model for analyzing the cascading failure process on an interdependent power-communication network that reflects interdependency's beneficial and adverse effects. We consider the nature of flow distribution in the layers and the structure and constraints of each network. We suggest an automatic load balancing mechanism that relies on facilitated controllability by the communication layer to switch off loads and generations. This scheme mitigates the density of severe cascading scenarios resulting from controllability loss after random failures, considering the immediate shedding load and lines' congestions. We investigate the effect of weak and strong interdependencies, the robustness of the communication network, and the coupling coefficient in different scenarios. We find that interdependency's beneficial and adverse effects vary in these scenarios, concluding that interdependency is beneficial under certain conditions.

Acknowledgments

A. Ghasemi gratefully acknowledges funding from the Alexander von Humboldt Foundation (Ref. 3.4 - IRN - 1214645 - GF-E) for his visiting research at the University of Passau in Germany.

References

[1] H. He and J. Yan, "Cyber-physical attacks and defences in the smart grid: a survey," *IET Cyber-Physical Systems: Theory & Applications*, vol. 1, no. 1, pp. 13–27, 2016.

[2] Y. Mo, T. H.-J. Kim, K. Brancik, D. Dickinson, H. Lee, A. Perrig, and B. Sinopoli, "Cyber–physical security of a smart grid infrastructure," *Proceedings of the IEEE*, vol. 100, no. 1, pp. 195–209, 2011.

[3] S. V. Buldyrev, R. Parshani, G. Paul, H. E. Stanley, and S. Havlin, "Catastrophic cascade of failures in interdependent networks," *Nature*, vol. 464, no. 7291, pp. 1025–1028, 2010.

[4] V. Rosato, L. Issacharoff, F. Tiriticco, S. Meloni, S. Porcellinis, and R. Setola, "Modelling interdependent infrastructures using interacting dynamical models," *International Journal of Critical Infrastructures*, vol. 4, no. 1-2, pp. 63–79, 2008.

[5] M.-E. Paté-Cornell, M. Kuypers, M. Smith, and P. Keller, "Cyber risk management for critical infrastructure: a risk analysis model and three case studies," *Risk Analysis*, vol. 38, no. 2, pp. 226–241, 2018.

[6] C. D. Brummitt, R. M. D'Souza, and E. A. Leicht, "Suppressing cascades of load in interdependent networks," *Proceedings of the National Academy of Sciences*, vol. 109, no. 12, pp. E680–E689, 2012.

[7] J. M. Carlson and J. Doyle, "Complexity and robustness," *Proceedings of the national academy of sciences*, vol. 99, no. suppl 1, pp. 2538–2545, 2002.

[8] A. E. Motter and Y. Yang, "The unfolding and control of network cascades," *arXiv preprint arXiv:1701.00578*, 2017.

[9] H. Haes Alhelou, M. E. Hamedani-Golshan, T. C. Njenda, and P. Siano, "A survey on power system blackout and cascading events: Research motivations and challenges," *Energies*, vol. 12, no. 4, p. 682, 2019.

[10] J. Bialek, E. Ciapessoni, D. Cirio, E. Cotilla-Sanchez, C. Dent, I. Dobson, P. Henneaux, P. Hines, J. Jardim, S. Miller *et al.*, "Benchmarking and validation of cascading failure analysis tools," *IEEE Transactions on Power Systems*, vol. 31, no. 6, pp. 4887–4900, 2016.

[11] R. Parshani, S. V. Buldyrev, and S. Havlin, "Interdependent networks: Reducing the coupling strength leads to a change from a first to second order percolation transition," *Physical review letters*, vol. 105, no. 4, p. 048701, 2010.

[12] B. A. Carreras, D. E. Newman, P. Gradney, V. E. Lynch, and I. Dobson, "Interdependent risk in interacting infrastructure systems," in *2007 40th Annual Hawaii International Conference on System Sciences (HICSS'07)*. IEEE, 2007, pp. 112–112.

[13] J. Shao, S. V. Buldyrev, S. Havlin, and H. E. Stanley, "Cascade of failures in coupled network systems with multiple support-dependence relations," *Physical Review E*, vol. 83, no. 3, p. 036116, 2011.

[14] A. Bashan, Y. Berezin, S. V. Buldyrev, and S. Havlin, "The extreme vulnerability of interdependent spatially embedded networks," *Nature Physics*, vol. 9, no. 10, pp. 667–672, 2013.

[15] D. T. Nguyen, Y. Shen, and M. T. Thai, "Detecting critical nodes in interdependent power networks for vulnerability assessment," *IEEE Transactions on Smart Grid*, vol. 4, no. 1, pp. 151–159, 2013.

[16] C. M. Schneider, N. Yazdani, N. A. Araújo, S. Havlin, and H. J. Herrmann, "Towards designing robust coupled networks," *Scientific reports*, vol. 3, p. 1969, 2013.

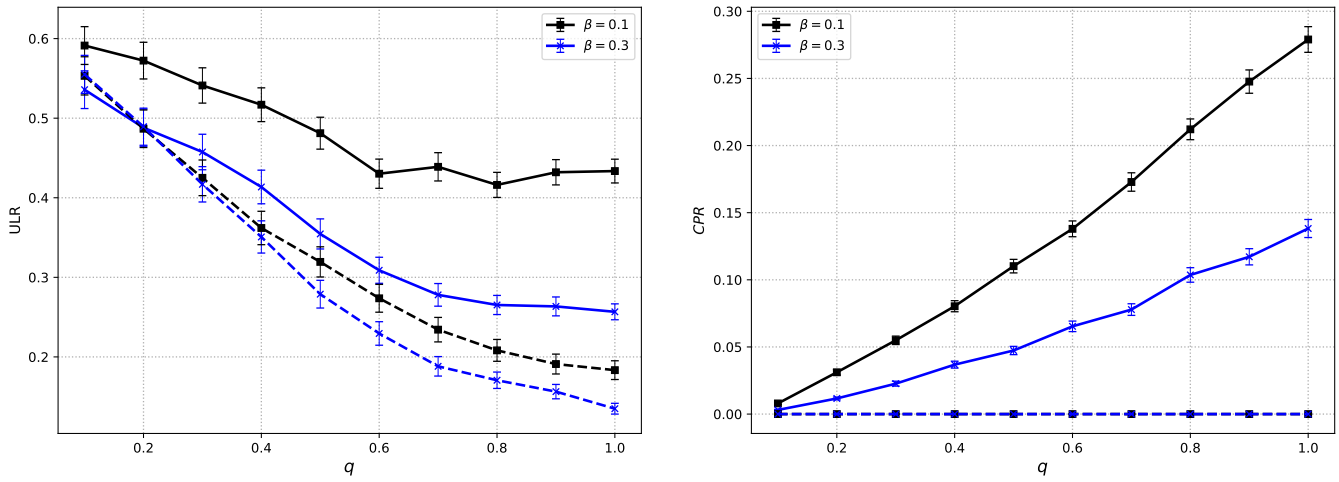

(a) (b)

Fig. 5: The average and the corresponding 95% confidence interval of (a) ULR and (b) CPR metric, against coupling coefficient for $\beta = 0.1, 0.3$ in the IEEE-118-Bus. The dashed lines are for the weak model, and the solid lines are for the strong model.

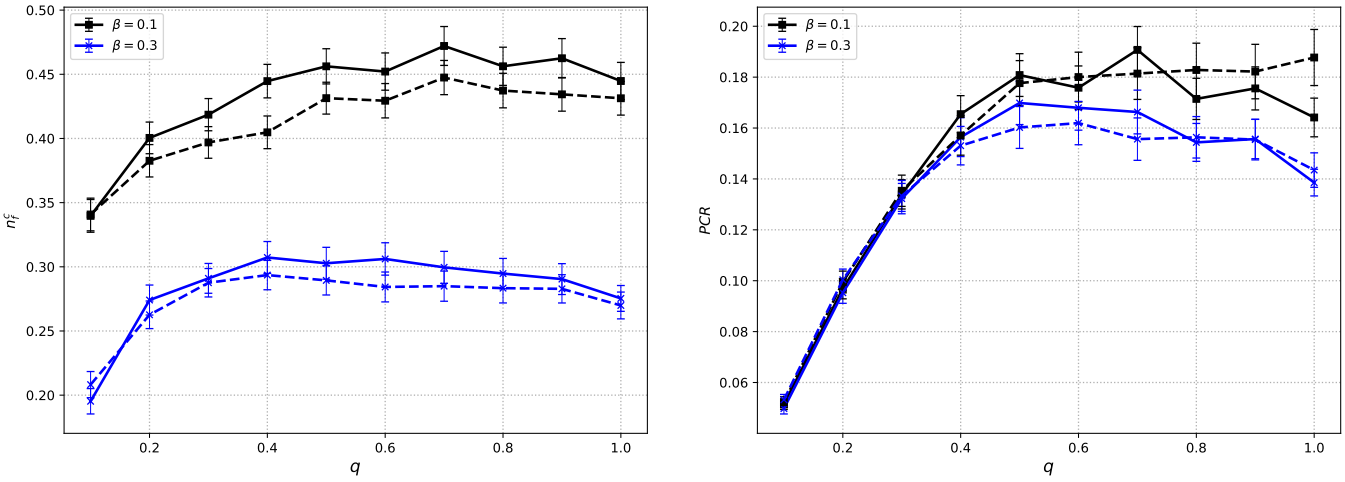

(a) (b)

Fig. 6: The average and the corresponding 95% confidence interval of (a) PCFN and (b) PCR metrics against the coupling coefficient for $\beta = 0.1, 0.3$ for the IEEE-118-Bus. The dashed lines are for the weak model, and the solid lines are for the strong model.

[17] M. Turalska, K. Burghardt, M. Rohden, A. Swami, and R. M. D'Souza, "Cascading failures in scale-free interdependent networks," *Physical Review E*, vol. 99, no. 3, p. 032308, 2019.

[18] H. Khamfroush, N. Bartolini, T. F. La Porta, A. Swami, and J. Dillman, "On propagation of phenomena in interdependent networks," *IEEE Transactions on network science and engineering*, vol. 3, no. 4, pp. 225–239, 2016.

[19] P. D. Hines, I. Dobson, and P. Rezaei, "Cascading power outages propagate locally in an influence graph that is not the actual grid topology," *IEEE Transactions on Power Systems*, vol. 32, no. 2, pp. 958–967, 2016.

[20] M. Korkali, J. G. Veneman, B. F. Tivnan, J. P. Bagrow, and P. D. Hines, "Reducing cascading failure risk by increasing infrastructure network interdependence," *Scientific reports*, vol. 7, p. 44499, 2017.

[21] A. Vespignani, "The fragility of interdependency," *Nature*, vol. 464, no. 7291, pp. 984–985, 2010.

[22] A. Sturaro, S. Silvestri, M. Conti, and S. K. Das, "A realistic model for failure propagation in interdependent cyber-physical systems," *IEEE Transactions on Network Science and Engineering*, vol. 7, no. 2, pp. 817–831, 2018.

[23] U. Nakarmi, M. Rahnamay-Naeini, and H. Khamfroush, "Critical component analysis in cascading failures for power grids using community structures in interaction graphs," *IEEE Transactions on Network Science and Engineering*, vol. 7, no. 3, pp. 1079–1093, 2019.

[24] Z. Chen, J. Wu, Y. Xia, and X. Zhang, "Robustness of interde-

pendent power grids and communication networks: A complex network perspective," *IEEE Transactions on Circuits and Systems II: Express Briefs*, vol. 65, no. 1, pp. 115–119, 2017.
[25] Y. Chen, Y. Li, W. Li, X. Wu, Y. Cai, Y. Cao, and C. Rehtanz, "Cascading failure analysis of cyber physical power system with multiple interdependency and control threshold," *IEEE Access*, vol. 6, pp. 39 353–39 362, 2018.
[26] X. Zhang, D. Liu, C. Zhan, and K. T. Chi, "Effects of cyber coupling on cascading failures in power systems," *IEEE Journal on Emerging and Selected Topics in Circuits and Systems*, vol. 7, no. 2, pp. 228–238, 2017.
[27] D. Z. Tootaghaj, N. Bartolini, H. Khamfroush, T. He, N. R. Chaudhuri, and T. La Porta, "Mitigation and recovery from cascading failures in interdependent networks under uncertainty," *IEEE Transactions on Control of Network Systems*, vol. 6, no. 2, pp. 501–514, 2018.
[28] M. Parandehgheibi and E. Modiano, "Robustness of interdependent networks: The case of communication networks and the power grid," in *2013 IEEE Global Communications Conference (GLOBECOM)*. IEEE, 2013, pp. 2164–2169.
[29] M. Vaiman, K. Bell, Y. Chen, B. Chowdhury, I. Dobson, P. Hines, M. Papic, S. Miller, and P. Zhang, "Risk assessment of cascading outages: Methodologies and challenges," *IEEE Transactions on Power Systems*, vol. 27, no. 2, p. 631, 2012.
[30] A. E. Motter and Y.-C. Lai, "Cascade-based attacks on complex networks," *Physical Review E*, vol. 66, no. 6, p. 065102, 2002.
[31] P. Hines, E. Cotilla-Sanchez, and S. Blumsack, "Topological models and critical slowing down: Two approaches to power system blackout risk analysis," in *2011 44th Hawaii International Conference on System Sciences*. IEEE, 2011, pp. 1–10.
[32] Y. Yang, T. Nishikawa, and A. E. Motter, "Vulnerability and cosusceptibility determine the size of network cascades," *Physical review letters*, vol. 118, no. 4, p. 048301, 2017.
[33] A. Plietzsch, P. Schultz, J. Heitzig, and J. Kurths, "Local vs. global redundancy–trade-offs between resilience against cascading failures and frequency stability," *The European Physical Journal Special Topics*, vol. 225, no. 3, pp. 551–568, 2016.
[34] B. A. Carreras, V. E. Lynch, I. Dobson, and D. E. Newman, "Critical points and transitions in an electric power transmission model for cascading failure blackouts," *Chaos: An interdisciplinary journal of nonlinear science*, vol. 12, no. 4, pp. 985–994, 2002.
[35] B. Stott, J. Jardim, and O. Alsaç, "Dc power flow revisited," *IEEE Transactions on Power Systems*, vol. 24, no. 3, pp. 1290–1300, 2009.
[36] S. Soltan, D. Mazauric, and G. Zussman, "Cascading failures in power grids: analysis and algorithms," in *Proceedings of the 5th international conference on Future energy systems*, 2014, pp. 195–206.
[37] J. Mohammadi and F. B. Ajaei, "Versatile decentralised control of the dc microgrid," *IET Smart Grid*, vol. 2, no. 1, pp. 77–88, 2019.
[38] N. N. A. Bakar, M. Y. Hassan, M. F. Sulaima, M. Na'im Mohd Nasir, and A. Khamis, "Microgrid and load shedding scheme during islanded mode: A review," *Renewable and Sustainable Energy Reviews*, vol. 71, pp. 161–169, 2017.
[39] D. Z. Tootaghaj, N. Bartolini, H. Khamfroush, and T. La Porta, "Controlling cascading failures in interdependent networks under incomplete knowledge," in *2017 IEEE 36th Symposium on Reliable Distributed Systems (SRDS)*. IEEE, 2017, pp. 54–63.
[40] J. Yan, Y. Tang, H. He, and Y. Sun, "Cascading failure analysis with dc power flow model and transient stability analysis," *IEEE Transactions on Power Systems*, vol. 30, no. 1, pp. 285–297, 2014.
[41] J. Mohammadi and F. B. Ajaei, "Dc microgrid load shedding schemes," in *2019 IEEE/IAS 55th Industrial and Commercial Power Systems Technical Conference (I&CPS)*. IEEE, 2019, pp. 1–7.
[42] N. Sapari, H. Mokhlis, J. A. Laghari, A. Bakar, and M. Dahalan, "Application of load shedding schemes for distribution network connected with distributed generation: A review," *Renewable and Sustainable Energy Reviews*, vol. 82, pp. 858–867, 2018.
[43] Q. Zhou, Z. Li, Q. Wu, and M. Shahidehpour, "Two-stage load shedding for secondary control in hierarchical operation of islanded microgrids," *IEEE Transactions on Smart Grid*, vol. 10, no. 3, pp. 3103–3111, 2018.
[44] L. Trigueiro dos Santos, M. Sechilariu, and F. Locment, "Optimized load shedding approach for grid-connected dc microgrid systems under realistic constraints," *Buildings*, vol. 6, no. 4, p. 50, 2016.
[45] L. Cuadra, S. Salcedo-Sanz, J. Del Ser, S. Jiménez-Fernández, and Z. W. Geem, "A critical review of robustness in power grids using complex networks concepts," *Energies*, vol. 8, no. 9, pp. 9211–9265, 2015.
[46] "IEEE 118 Bus and 300 bus test cases," https://matpower.org/docs/ref/matpower5.0/case118.html, https://matpower.org/docs/ref/matpower5.0/case300.html, [Online; accessed 4-August-2022].

Abdorasoul Ghasemi is with the Faculty of Computer Engineering of K.N. Toosi University of Technology, Tehran, Iran. He received his Ph.D. and M.Sc. degrees from Amirkabir University of Technology (Tehran Polytechnique), Tehran, Iran, and his B.Sc. from the Isfahan University of Technology, all in Electrical Engineering. He has spent sabbatical leaves with the computer science department at the University of California, Davis, CA, the USA (April 2017 to August 2018) and Max Planck Institute for the physics of complex systems, Dresden, Germany (Dec. 2020 to July 2021). He has been awarded the Alexander von Humboldt fellowship for experienced researchers in July 2021, working on resilient cyber-physical energy systems at the University of Passau, Germany. His research interests include network science and its engineering applications, including communications, energy, and cyber-physical systems using optimization and machine learning approaches.

Hermann de Meer received the Ph.D. degree in computer science from the University of Erlangen-Nuremberg, Germany. He held Post-Doctoral Research positions at Hamburg University, Germany, University of Texas at Austin, USA, Duke University, USA, and Columbia University, USA. After his Readership at University College London (UCL), U.K., he was appointed as Professor at Passau University, Germany, in 2003. His area of research comprises computer networking and energy systems with special focus on network virtualization, IT-security of the smart grid, demand side management, E-Mobility, industry automation, and resilience and risk management of distributed systems.

Supplementary material
Robustness of interdependent power grid and communication networks to cascading failures

Abdorasoul Ghasemi and Hermann de Meer

S.1 FAILURE CASCADING IN COMMUNICATION LAYER

This section provides more details about the failure cascading model in the communication layer. We start by discussing how to generate topology and find the nominal load of each node. Then, we explain adjusting the nodes' capacities according to their nominal load by discussing how a source and destination could effectively communicate in a timely manner.

We do not have the actual topology and the nodes' capacities of the communication network. We assume that the communication network has the same number of nodes as the corresponding power network. Its topology is generated by randomly rewiring 10% of the power network and randomly adding 10% more edges to this graph. The reason is that the communication network typically co-evolves with the power layer.

To determine the capacity of the nodes more realistically, we first find the nominal load of each node and then consider the node capacity proportional to it. We find the number of shortest paths passing through each node to estimate its nominal load, i.e., the node's betweenness centrality measure. Using the betweenness centrality measure is effectively the same as assuming some background communications between the other node pairs, i.e., there is a one-unit information exchange between nodes. Note that we use this assumption to find the capacity of each node where a coupled bus is observable if there is a congestion-free path between the control center and the corresponding coupled node.

In packet-switched networks, routing protocol determines the path packets traverse to reach their destination. We use the shortest path as the routing protocol, and the destination is the control center. Consider a node in the path of a given source node to the control center. The arrived data packets are queued in each intermediate node's output buffer to forward to the next hop on the path. The observed average queueing delay, T, generally depends on packets' arrival and service rates stochastic processes. For example, in the *M/M/1* queueing model, packets arrive according to the Poisson process with the rate λ and the probability distribution of service time, i.e., the ratio of random packet length to the output link rate, is exponential with mean $1/\mu$ sec we have $T = \frac{1}{\mu-\lambda} = \frac{\rho}{\lambda(1-\rho)}$, where $\rho = \frac{\lambda}{\mu}$. The average delay tends to infinity if the link's utilization tends to one. The corresponding output buffer will be congested if the offered load to an output link exceeds a certain threshold. In regular operation, the load of each link is far away from the congestion region. Therefore, as in Equ. (1) of the main text, we could consider a tolerance coefficient to consider the excessive load the link node can forward without excessive delay.

S.2 SIMULATION RESULTS FOR IEEE-300-BUS NETWORK

This section provides the simulation results for the robustness evaluation of the interdependent IEEE-300-bus network.

S.2.1 Congestion aware load balancing

We generate 5 instances of the IEEE-300 bus transmission power network, consider 5 random rewiring between the layers, and measure the unserved load ratio for a pre-determined 100 random line failure scenarios with $q = 0.5$, $\beta = 0.3$, and $f = 0.01$. We set $P_1 = 1$ and $P_2 = 10$ in congestion-aware load balancing.

Fig. S1 shows the density function of the corresponding ULR for congestion-aware load balancing ($\mu_1 = 0.8, \mu_2 = 0.4$) against the scenario which does not consider lines' congestions ($\mu_1 = 1.0, \mu_2 = 0$) for strong and weak interdependent models. In both models considering the lines' congestions in the load balancing decreases the average unserved load by decreasing the density of severe cascades. Here for the strong model, the ULR is decreased from 0.43 to 0.4, and for the weak interdependency model, from 0.34 to 0.27.

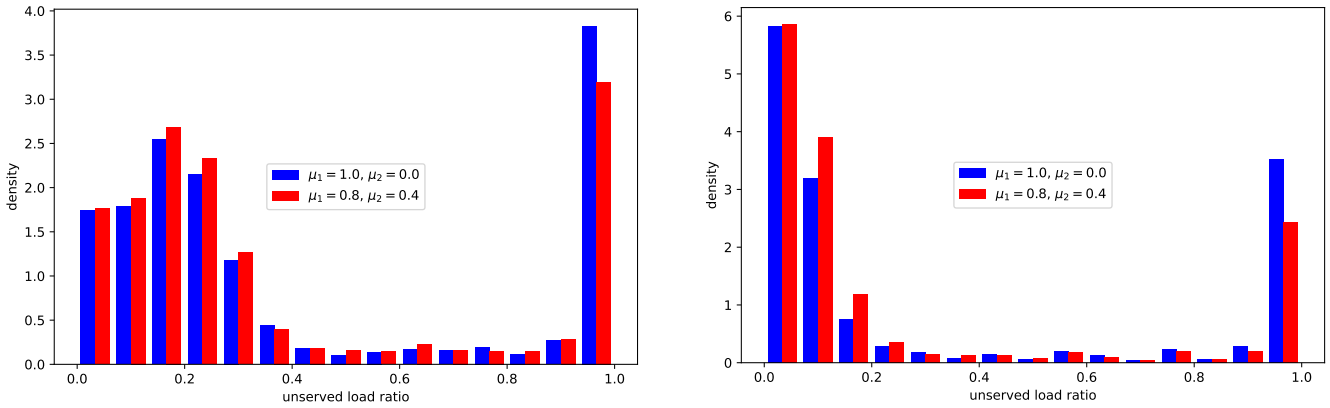

(a) (b)

Fig. S1: The density function of the unserved load ratio without ($\mu_1 = 1.0, \mu_2 = 0$) and with ($\mu_1 = 0.8, \mu_2 = 0.4$) consideration of lines congestions for (a) strong interdependency and (b) weak interdependency models in IEEE-300 Bus network.

S.2.2 Robustness against random failures

Here we provide the results of IEEE-300-bus network robustness against random failure cascading. The result for each f is the average of running the process for 5 instances of power network at different loads and 5 instances for the corresponding communication network. We randomly chose 5 distinctive sets of couplings between the nodes of two layers for each pair of these power and communication networks according to the coupling coefficient q to construct the interdependent network. Finally, we simulate the process 5 times by randomly removing a fraction f of lines. Accordingly, the results are the average of 625 distinct scenarios with different loads, communication network topology, coupling patterns, and failure scenarios for each point. Fig. S2 shows the corresponding unserved load ratio and giant component size against different values of f.

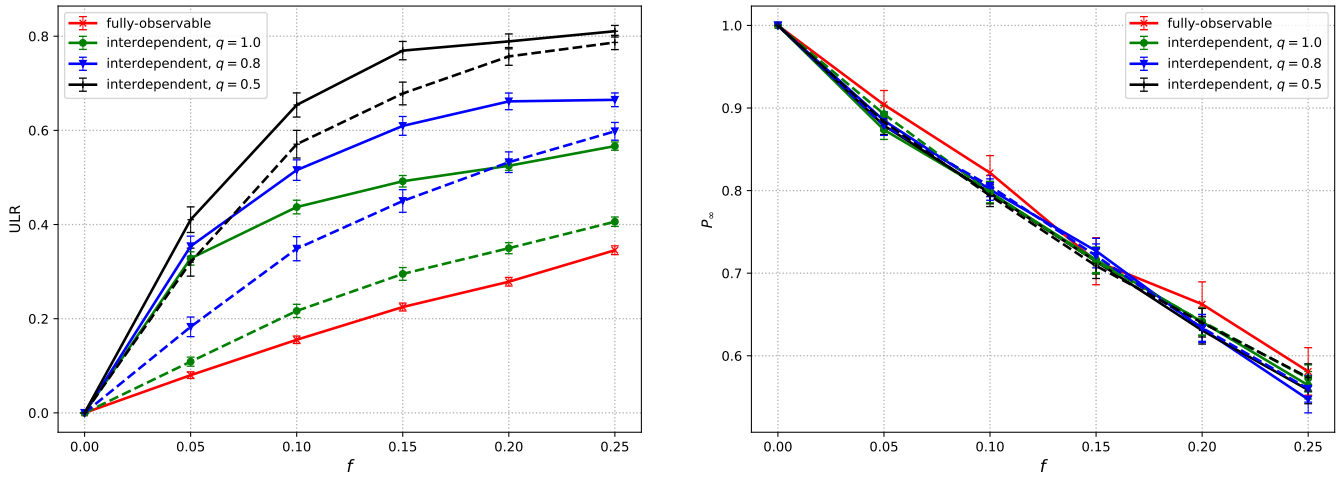

(a) (b)

Fig. S2: The average and the corresponding 95% confidence interval of ULR and giant component size P_∞ against the fraction of randomly failed edges for the IEEE-300-Bus for $\beta = 0.3$. The dashed lines are for the weak model and the solid lines are for the strong model.

S.2.3 The effect of coupling coefficient

This section provides the results of robustness metrics against the coupling coefficient. We use the same simulation setup in subsection S.2.2 and assume $f = 0.01$ fraction of lines are randomly failed.

Fig. S3 shows the ULR and CPR metrics. Fig. S4(a) and Fig. S3(b) show, respectively, the total fraction of failed communication nodes and the fraction of failed nodes due to the failure rollover from the power network.

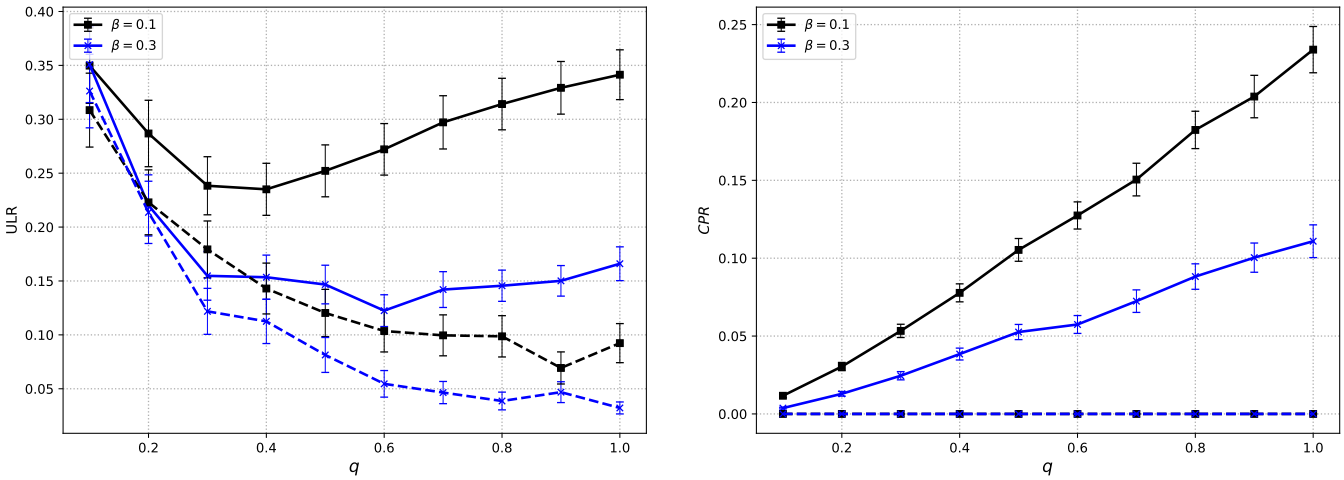

(a) (b)

Fig. S3: The average and the corresponding 95% confidence interval of ULR and the CPR metric against the coupling coefficient for $\beta = 0.1, 0.3$ for the IEEE-300-Bus. The dashed lines are for the weak model and the solid lines are for the strong model.

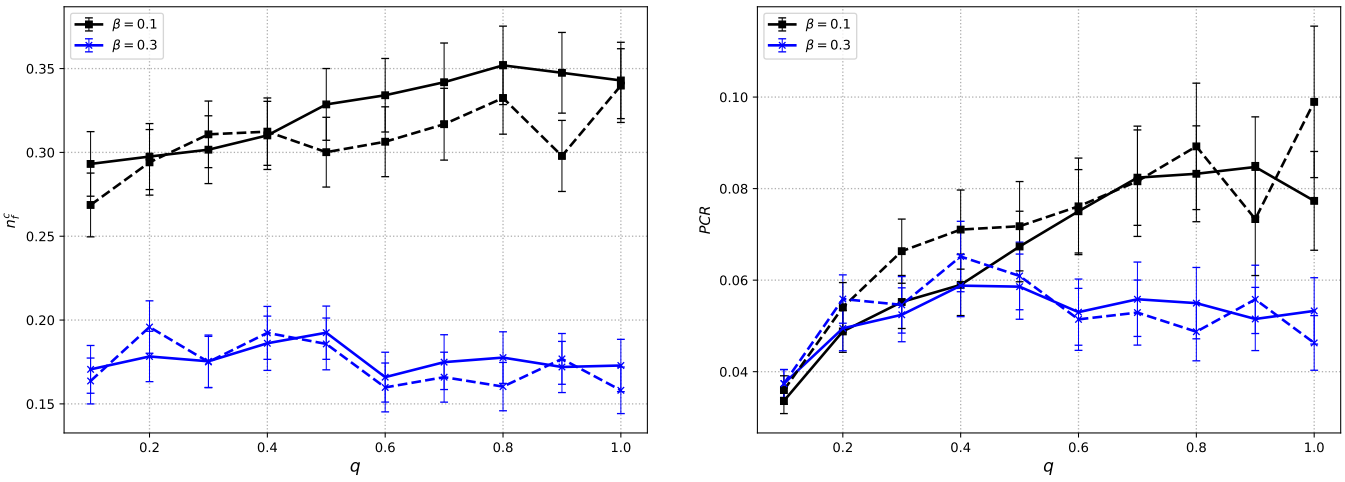

(a) (b)

Fig. S4: The average and the corresponding 95% confidence interval of PCFN and PCR metrics against the coupling coefficient for $\beta = 0.1, 0.3$ for the IEEE-300-Bus. The dashed lines are for the weak model and the solid lines are for the strong model.